PHYSICAL REVIEW D **94,** 085010 (2016)

Casimir self-entropy of an electromagnetic thin sheet

Yang Li,[1,*] Kimball A. Milton,[1,†] Pushpa Kalauni,[1,‡] and Prachi Parashar[1,2,3,§]
[1]*H. L. Dodge Department of Physics and Astronomy, University of Oklahoma, Norman, Oklahoma 73019, USA*
[2]*Department of Physics, Southern Illinois University–Carbondale, Carbondale, Illinois 62091, USA*
[3]*Department of Energy and Process Engineering, Norwegian University of Science and Technology, 7491 Trondheim, Norway*
(Received 22 July 2016; published 13 October 2016)

Casimir entropies due to quantum fluctuations in the interaction between electrical bodies can often be negative, caused either by dissipation or by geometry. Although generally such entropies vanish at zero temperature, consistent with the third law of thermodynamics (the Nernst heat theorem), there is a region in the space of temperature and separation between the bodies where negative entropy occurs, while positive interaction entropies arise for large distances or temperatures. Systematic studies on this phenomenon in the Casimir-Polder interaction between a polarizable nanoparticle or atom and a conducting plate in the dipole approximation have been given recently. Since the total entropy should be positive according to the second law of thermodynamics, we expect that the self-entropy of the bodies would be sufficiently positive as to overwhelm the negative interaction entropy. This expectation, however, has not been explicitly verified. Here we compute the self-entropy of an electromagnetic δ-function plate, which corresponds to a perfectly conducting sheet in the strong coupling limit. The transverse electric contribution to the self-entropy is negative, while the transverse magnetic contribution is larger and positive, so the total self-entropy is positive. However, this self-entropy vanishes in the strong-coupling limit. In that case, it is the self-entropy of the nanoparticle, which we recalculate in the perfect conducting limit, that is just sufficient to result in a non-negative total entropy.

DOI: 10.1103/PhysRevD.94.085010

I. INTRODUCTION

Negative Casimir entropies were first encountered in modeling the electrical properties of a metal plate including dissipation due to finite conductivity [1–3]. It was found that although the Nernst heat theorem is satisfied, in that the entropy vanishes as the temperature approaches zero, signaling the existence of a single ground state, there was an intermediate region of separation between two metal plates and of temperature in which the entropy was negative. It was argued that this was of no serious concern, although perhaps surprising, because it is only the total entropy, which includes the self-entropies of the two bodies and that of the environment, that must be positive.

Somewhat later, it was noticed that negative Casimir entropies also emerged geometrically even for dissipationless materials. For example, negative entropy occurred in the interaction between polarizable atoms and conducting plates [4]. The same phenomenon was observed between a perfectly conducting sphere and a perfectly conducting plane [5,6], and between two perfectly conducting spheres [7,8]. The negative entropy phenomenon was dominated by the dipole approximation, already in the single-scattering approximation, which led to systematic studies on the effect for the Casimir-Polder interaction between an anisotropic polarizable atom or nanoparticle and a conducting plate, or between two such nanoparticles [9–11]. The appearance of negative entropy was common, nearly ubiquitous, even between perfect conductors, as shown in Fig. 1 taken from Ref. [12]. Here we see the interaction entropy between a sphere and a plane, and between two identical spheres, calculated in the single-scattering dipole approximation. When the separation distance Z times the temperature T is of order unity (in natural units), there is a region where the entropy is negative. For the sphere-sphere case at room temperature, the entropy is most negative at a readily measurable distance of a few μm. The behavior of the perfectly conducting sphere-plate entropy for small separations is

$$S_{\mathrm{Sph-Pl}}(T) \sim -\frac{4}{15}(\pi a T)^3, \qquad 4\pi Z T \ll 1, \quad (1.1)$$

where a is the radius of the sphere.

Again, the supposition was that although this negative entropy region is surprising, it does not violate any fundamental physical principle, because it is compensated by larger effects, such as the entropy of the vacuum and that due to the bodies themselves. The purpose of this paper is to investigate the latter, which has many interesting features

*liyang@ou.edu
†kmilton@ou.edu
‡pushpa@ou.edu
§prachi@nhn.ou.edu

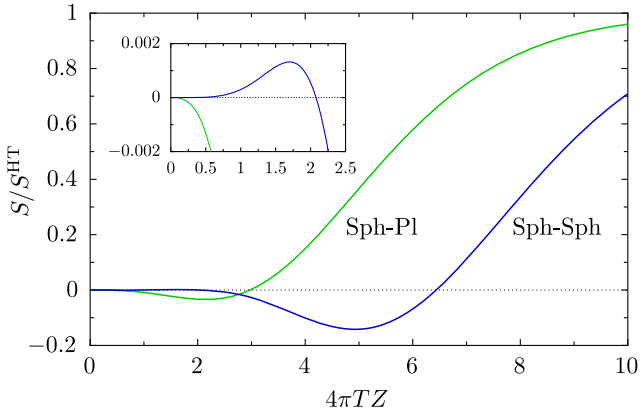

FIG. 1. The entropy of interaction between a perfectly conducting sphere and a perfectly conducting plane (Sph-Pl) and between two perfectly conducting spheres (Sph-Sph) normalized with respect to the corresponding high-temperature values is displayed as a function of the product of distance Z and temperature T. The entropy has been evaluated within the dipole and single-scattering approximation [12]; the ratio of entropies is independent of the radii of the spheres. The inset shows the behavior of the entropy for small TZ. We call the negative entropy region perturbative for the sphere-plane configuration and nonperturbative for the sphere-sphere configuration.

in its own right. The self-energy of a body possesses many well-known divergences, as does the free energy of a body at finite temperature, but the entropy should be finite and unambiguous. How this comes about is nontrivial and certainly the sign cannot be ascertained *a priori*.

A model for a thin conducting plate, which we call an electromagnetic δ-function plate [13], is considered in Sec. II. In the strong coupling limit, this corresponds to a perfectly conducting surface with zero skin depth. In Sec. III, we investigate the strong and weak coupling limits of the entropy, which are analyzed in more detail in Sec. IV where we calculate the transverse electric (TE) and transverse magnetic (TM) contributions separately. For this end, we adopt a plasma model for the dispersive character of the coupling. Although it is not analytic at the origin, we obtain the TE part of the free energy by expanding in powers of the coupling (weak coupling expansion). The entropy, unlike the free energy, is finite and is expressed in terms of an explicit function of the coupling divided by the temperature. In contrast, for the TM part, the natural expansion is in inverse powers of the coupling (strong coupling expansion). Again, a finite closed-form expression for the entropy emerges. The results are that the TE contribution to the entropy (which corresponds to a scalar δ-function plate—a Dirichlet plate in strong coupling) is always negative, while the TM contribution is always positive and larger than the magnitude of the TE part. The total self-entropy of the plate is thus positive, except in the strong-coupling limit, where the sum of the two terms vanishes. The more realistic Drude model for dispersion is then briefly discussed. Since the entropy of the plates vanishes in strong coupling, we compute, in Sec. V, the self-entropies of a polarizable particle. When this is realized as a conducting sphere, the negative entropy found in the interaction between a perfectly conducting sphere and a plane is exactly canceled. The general problem of the entropy of an electromagnetic δ-function sphere will be treated in a subsequent publication. Some concluding remarks are offered in Sec. VI. In this paper, we utilize a point-splitting regulation method, which is illustrated in the Appendix by reconsidering the old problem [14] of the vacuum expectation value of the stress tensor in empty Minkowski space.

We use natural units $\hbar = c = k_B = 1$ and Heaviside-Lorentz electromagnetic units except for the polarizabilities which are in Guassian units.

II. ELECTROMAGNETIC δ-FUNCTION PLATE

We start from the general expression for the free energy with the vacuum energy subtracted,

$$F = -\frac{T}{2}\sum_{m=-\infty}^{\infty} \mathrm{Tr}\ln \mathbf{\Gamma}\mathbf{\Gamma}_0^{-1}, \tag{2.1}$$

where the trace is over spatial coordinates and internal variables (tensor indices). The trace depends on the imaginary Matsubara frequency $\zeta_m = 2\pi m T$. The Green's dyadic $\mathbf{\Gamma}$ satisfies

$$\left[-\frac{1}{\zeta_m^2}\boldsymbol{\nabla}\times\boldsymbol{\nabla}\times -\boldsymbol{\varepsilon}(i\zeta_m)\right]\mathbf{\Gamma} = \mathbf{1}\delta(\mathbf{r}-\mathbf{r}'), \tag{2.2}$$

$\mathbf{\Gamma}_0$ is the free Green's dyadic, and $\boldsymbol{\varepsilon}$ is the permittivity tensor of the anisotropic medium. Identifying the potential $\mathbf{V} = \boldsymbol{\varepsilon} - \mathbf{1}$, the free energy is

$$F = \frac{T}{2}\sum_{m=-\infty}^{\infty} \mathrm{Tr}\ln(\mathbf{1} - \mathbf{\Gamma}_0\mathbf{V}). \tag{2.3}$$

Here, we consider an anisotropic δ-function plate, where

$$\mathbf{V} = \boldsymbol{\lambda}\delta(z) = \mathrm{diag}(\lambda_\perp, \lambda_\perp, \lambda_z)\delta(z). \tag{2.4}$$

In Ref. [13] we showed that λ_z must be set equal to zero in accordance with Maxwell's equations.[1] We, therefore, write $\lambda = \lambda_\perp$, which could be a function of the imaginary frequency ζ. In this approach all we need is the free Green's dyadic, written in this transverse description,

[1]This has been disputed by Barton [15] and Bordag [16]. In our case, the value of the normal component of the coupling does not occur in the expression for the free energy.

$$\mathbf{\Gamma}_0(\mathbf{r},\mathbf{r}') = \int \frac{(d\mathbf{k}_\perp)}{(2\pi)^2} e^{i\mathbf{k}_\perp\cdot(\mathbf{r}-\mathbf{r}')_\perp}\boldsymbol{\gamma}_0,$$
$$\boldsymbol{\gamma}_0 = (\mathbf{E}+\mathbf{H})g_0,$$
$$g_0(z,z') = \frac{1}{2\kappa_m}e^{-\kappa_m|z-z'|}, \tag{2.5}$$

where $\kappa_m = \sqrt{k^2+\zeta_m^2}$, g_0 is the free reduced Green's function, while $\mathbf{E}$ and $\mathbf{H}$ are the polarization dyadic operators for the TE and TM modes, respectively. Because $\mathbf{V}$ is a diagonal matrix in the transverse sector, the polarization operators are effectively trivial. In the coordinate system where $\mathbf{k}_\perp$ lies along the x axis,

$$\mathbf{VE} = -\lambda\delta(z)\zeta^2\begin{pmatrix}0&0\\0&1\end{pmatrix}, \qquad \mathbf{VH} = \lambda\delta(z)\begin{pmatrix}1&0\\0&0\end{pmatrix}\partial_z\partial_{z'}, \tag{2.6}$$

which are orthogonal. Expanding the logarithm in the free energy (2.3), and regulating the divergent sum and integral by point splitting in imaginary time τ and transverse space δ, as in several recent papers [17–19], yields the free energy per unit area

$$F = -\frac{T}{4\pi}\sum_{m=-\infty}^{\infty} e^{i\zeta_m\tau} \times \int_0^\infty dk\,k J_0(k\delta)\left[\ln\frac{2}{2+\lambda\kappa_m}+\ln\frac{2\kappa_m}{2\kappa_m+\lambda\zeta_m^2}\right], \tag{2.7}$$

where the first term is the TM contribution and the second is the TE contribution. It is understood that the regulators τ and δ are set to zero at the end of the calculation. The structures appearing in the logarithms are the TM and TE transmission coefficients, also expressible in terms of reflection coefficients,

$$t^E = \frac{1}{1+\lambda\zeta_m^2/(2\kappa_m)} = 1+r^E, \qquad t^H = \frac{1}{1+\lambda\kappa_m/2} = 1-r^H. \tag{2.8}$$

III. ASYMPTOTIC COUPLING BEHAVIORS

A. Strong coupling limit

It is illuminating, as we shall see in the next section, to examine the contributions of the TE and TM modes separately. But the composite structure evidently possesses significant cancellations. So we first turn to strong coupling, $\lambda\to\infty$, which represents a perfect conductor. In that limit the two logarithms in Eq. (2.7) combine to give $2\ln(2/\lambda\zeta_m)$; that is, the κ_m dependence has canceled out. Then, according to

$$\int_0^\infty dk\,k J_0(k\delta) = 0, \qquad \delta\neq 0, \tag{3.1}$$

the free energy vanishes, which is not true for the TE and TM modes individually.

In the strong coupling limit, the TE mode term involves the integral

$$I(\zeta_m,\delta) = \int_0^\infty dk\,k J_0(k\delta)\ln\kappa_m = \frac{d}{d\alpha}\int_0^\infty dk\,k J_0(k\delta)(k^2+\zeta_m^2)^{\alpha/2}\Big|_{\alpha=0} = -\frac{|\zeta_m|}{\delta}K_1(|\zeta_m|\delta). \tag{3.2}$$

Of course, the integral given does not exist. However, the second integral does exist for $\alpha<-1/2$, so we evaluate it analytically there, differentiate with respect to α, and continue back to $\alpha=0$. The $m=0$ term is to be understood as a limit as $\zeta_m\to 0$. Alternatively, one gets the same result when integrating by parts and omitting the divergent surface term. This leads to the expression for the free energy in the strong-coupling limit

$$F^{\mathrm{TE}} = \frac{T}{2\pi\delta}\sum_{m=0}^{\infty}{}' |\zeta_m|K_1(|\zeta_m|\delta), \tag{3.3}$$

where the primed sum means the $m=0$ term is counted with half weight.

We can evaluate this by using the Euler-Maclaurin sum formula around $m=1$ (we cannot expand around $m=0$ since the summand is singular there). If we let $g(m) = z_m K_1(z_m)$, where $z_m=\zeta_m\delta$, the sum formula reads

$$\sum_{m=0}^{\infty}{}' g(m) = \frac{1}{2}g(0)+\frac{1}{2}g(1) + \int_1^\infty dm\,g(m) - \sum_{q=1}^{\infty}\frac{B_{2q}}{(2q)!}g^{(2q-1)}(1), \tag{3.4}$$

where the B_n are Bernoulli numbers. The first three terms on the right side of Eq. (3.4) are obvious, and the remainder sum in the Euler-Maclaurin formula (3.4) is asymptotic, which is evaluated by Borel summation according to Ref. [20],

$$\sum_{q=2}^{\infty}\frac{B_{2q}}{(2q)!}(2q-4)! = \frac{1}{2}\left[\frac{1}{36}-\frac{\zeta(3)}{4\pi^2}\right]. \tag{3.5}$$

When these components are added together, we get the free energy and entropy

$$F^{\mathrm{TE}} = \frac{1}{8\pi\delta^3}+\frac{\zeta(3)}{4\pi}T^3, \qquad S^{\mathrm{TE}} = -\frac{3}{4\pi}\zeta(3)T^2<0. \tag{3.6}$$

The TM strong-coupling entropy exactly cancels this according to Eq. (3.1), which is explicitly verified in Sec. IV B.

B. Weak coupling limit

In the weak coupling limit, $\lambda \to 0$, the free energy is approximated as

$$F = \frac{T}{4\pi} \sum_{m=-\infty}^{\infty} \int_0^\infty dk\, k J_0(k\delta) \frac{\lambda}{2} \left(\kappa_m + \frac{\zeta_m^2}{\kappa_m} \right), \tag{3.7}$$

where we only keep the $O(\lambda)$ terms of the combination of logarithms in Eq. (2.7). The integrals are easily carried out, leaving us with a single frequency summation,

$$F = -\frac{T}{4\pi\delta^3} \left(1 - \delta \frac{d}{d\delta} - \delta^2 \frac{d^2}{d\delta^2} \right) {\sum_{m=0}^{\infty}}' \lambda(i\zeta_m) \cos(\zeta_m \tau) e^{-\zeta_m \delta}. \tag{3.8}$$

Here we recall that the coupling λ could well be a function of frequency. We will at this point assume such dependence is absent (but see below) and temporarily set $\tau = 0$, since the sum converges without a temporal cutoff. Then we obtain the free energy per unit area F and entropy per unit area S

$$F = -\lambda \frac{\pi^2}{45} T^4, \qquad S = -\frac{\partial F}{\partial T} = \lambda \frac{4\pi^2}{45} T^3 > 0. \tag{3.9}$$

According to the above procedure, the TE and TM contributions are

$$F^{\mathrm{TE}} = \lambda \frac{T}{4\pi\delta} {\sum_{m=0}^{\infty}}' \zeta_m^2 e^{-\zeta_m \delta} = \frac{\lambda}{4\pi^2\delta^4} - \lambda \frac{\pi^2}{60} T^4 + O(\delta^2), \tag{3.10a}$$

$$F^{\mathrm{TM}} = -\lambda \frac{T}{4\pi\delta^3} {\sum_{m=0}^{\infty}}' (1 + \delta\zeta_m) e^{-\zeta_m \delta} = -\frac{\lambda}{4\pi^2\delta^4} - \lambda \frac{\pi^2}{180} T^4 + O(\delta^2). \tag{3.10b}$$

Now each component possesses a divergent free energy, but the entropy in both cases is positive, and the sum of the two modes yields the finite result (3.9).

It might seem more sensible to use something like a plasma or Drude model to describe the frequency dependence of the coupling λ. Suppose $\lambda = \lambda_0/\zeta_m^2$, where λ_0 is a constant. Then we get a different result for the weak-coupling TE contribution,

$$F^{\mathrm{TE}} = \frac{\lambda_0 T}{8\pi\delta} \coth \pi T\delta = \frac{\lambda_0}{8\pi^2\delta^2} + \frac{\lambda_0 T^2}{24} + O(\delta^2). \tag{3.11}$$

This yields a *negative* contribution to the entropy. There is no weak-coupling expansion for the TM mode (and, as we will see, not for the TE mode either) in the plasma model—see Sec. IV B below.

IV. FINITE COUPLING BEHAVIORS

A. Finite coupling–TE mode

Consider the free energy from the TE mode (which is the same as for a scalar field under the influence of a δ-function potential) with the plasma model $\lambda = \lambda_0/\zeta_m^2$, where λ_0 is constant. The Drude model, which includes dissipation, for room temperature effectively differs from the plasma model merely by the omission of the $m = 0$ mode from the Matsubara sum. According to Eq. (2.7) and the plasma model, F^{TE} is

$$F^{\mathrm{TE}} = \frac{T}{2\pi} {\sum_{m=0}^{\infty}}' \cos(\zeta_m \tau) \int_0^\infty dk\, k J_0(k\delta) \ln\left(1 + \frac{\lambda_0}{2\kappa_m} \right). \tag{4.1}$$

We cannot expand in λ_0 because the expansion is not valid at $m = 0$.

The $m = 0$ term in Eq. (4.1) is

$$F^{\mathrm{TE}}_{m=0} = \frac{T}{4\pi\delta^2} \int_0^\infty dx\, x J_0(x) \ln\left(1 + \frac{\lambda_0 \delta}{2x} \right). \tag{4.2}$$

When we integrate by parts, the surface term vanishes and we obtain an answer in terms of modified Bessel functions and Struve functions. All we need is the small δ behavior,

$$F^{\mathrm{TE}}_{m=0} \sim \frac{\lambda_0 T}{8\pi\delta} + \frac{\lambda_0^2 T}{32\pi} \left(\ln \frac{\lambda_0 \delta}{4} + \gamma - \frac{1}{2} \right), \tag{4.3}$$

plus corrections which vanish as $\delta \to 0$.

We expand the remainder of Eq. (4.1) to second order in λ_0 (as an example),

$$F^{\mathrm{TE}}_{m\neq 0} \approx \frac{T}{2\pi} \sum_{m=1}^{\infty} \cos(\zeta_m \tau) \left[\frac{\lambda_0}{2\delta} \int_0^\infty \frac{dx\, x J_0(x)}{\sqrt{x^2 + \zeta_m^2 \delta^2}} - \frac{\lambda_0^2}{8} \int_0^\infty \frac{dx\, x J_0(x)}{x^2 + \zeta_m^2 \delta^2} \right]. \tag{4.4}$$

The two integrals here give convergence factors for the remaining sum on m,

$$\int_0^\infty \frac{dx\, x J_0(x)}{\sqrt{x^2 + \zeta_m^2 \delta^2}} = e^{-|\zeta_m|\delta}, \qquad \int_0^\infty \frac{dx\, x J_0(x)}{x^2 + \zeta_m^2 \delta^2} = K_0(|\zeta_m|\delta). \tag{4.5}$$

The order λ_0 term is immediately evaluated in terms of a hyperbolic cotangent, expanded to read, when combined with the corresponding $m = 0$ term from Eq. (4.3),

$$F^{\rm TE}_{(1)} = \frac{\lambda_0}{8\pi^2}\frac{1}{\delta^2+\tau^2} + \frac{\lambda_0 T^2}{24}, \tag{4.6}$$

a slight generalization of Eq. (3.11). Since it seems that only the spatial cutoff plays an essential role, we will henceforth for simplicity set $\tau = 0$. The second-order term in Eq. (4.4) is just a sum of Macdonald functions, which is evaluated using the Euler-Maclaurin sum formula (3.4) and then the Borel summation as before. Including the $m = 0$ term from Eq. (4.3), the "second-order" term in the free energy is

$$F^{\rm TE}_{(2)} = -\frac{\lambda_0^2}{64\pi\delta} + \frac{\lambda_0^2 T}{32\pi}\left(\ln\frac{\lambda_0}{2T} - \frac{1}{2}\right). \tag{4.7}$$

Evidently the free energy is not analytic near the origin in either λ_0 or T.

An extension of this method allows us to get a closed form for the scalar or plasma-model TE free energy. First we integrate Eq. (4.1) by parts,

$$F^{\rm TE} = \frac{\lambda_0 T}{8\pi\delta}\sum_{m=-\infty}^{\infty}\int_0^\infty \frac{dx\, x^2 J_1(x)}{(x^2+\zeta_m^2\delta^2)(\sqrt{x^2+\zeta_m^2\delta^2}+\lambda\delta/2)}. \tag{4.8}$$

The $m = 0$ term is just that we found before, in Eq. (4.3). We expand the $m \neq 0$ terms in (4.8) in powers of $\lambda\delta/2$, and for the coefficient of $(\lambda\delta/2)^n$ use the integral

$$\int_0^\infty \frac{dx\, x^2 J_1(x)}{(x^2+y^2)^{(n+3)/2}} = \frac{|y|^{(1-n)/2}K_{(1-n)/2}(|y|)}{2^{(n+1)/2}\Gamma(\frac{n+3}{2})}, \qquad n > -\frac{3}{2}. \tag{4.9}$$

The first term ($n = 0$) in this expansion corresponds to the first-order term in Eq. (3.11), while the second term ($n = 1$) gives the second-order term in Eq. (4.7). The term with $n = 2$ gives an explicit logarithm. The higher terms are worked out again with the Euler-Maclaurin formula used for the sum on m. This allows us to evaluate for $n > 2$ for small ϵ

$$\sum_{m=1}^{\infty}(m\epsilon)^{(1-n)/2}K_{(n-1)/2}(m\epsilon) \sim \epsilon^{1-n}2^{(n-3)/2}\Gamma\left(\frac{n-1}{2}\right)\zeta(n-1), \tag{4.10}$$

which gives

$$F^{\rm TE} = \frac{\lambda_0}{8\pi^2\delta^2} - \frac{\lambda_0^2}{64\pi\delta} + \frac{\lambda_0 T^2}{24} + \frac{\lambda_0^2 T}{32\pi}\left(\ln\frac{\lambda_0}{2T} - \frac{1}{2}\right) - \frac{\lambda_0^3}{96\pi^2}\ln 2\pi T\delta + \frac{\lambda_0 T^2}{2}\sum_{n=3}^{\infty}(-1)^n\left(\frac{\lambda_0}{4\pi T}\right)^n\frac{\zeta(n-1)}{n^2-1}. \tag{4.11}$$

The sum on n here can be carried out in terms of the generalized or Hurwitz zeta function. Although the free energy is divergent, what is of most interest is the finite self-entropy,

$$S^{\rm TE} = -\frac{\partial}{\partial T}F^{\rm TE} = \frac{\lambda_0^2}{16\pi}s^{\rm TE}(x), \qquad x = \frac{\lambda_0}{4\pi T}, \tag{4.12}$$

where we define a dimensionless entropy $s^{\rm TE}(x)$. The two alternative forms for $s^{\rm TE}$ are

$$s^{\rm TE}(x) = \frac{1}{2} - \frac{1}{6x} + \frac{2x}{3} - \frac{\ln x}{2} - \frac{3\zeta(3)}{4\pi^2x^2} - \frac{3}{x^2}\zeta^{(1,0)}(-2,1+x) + \frac{4}{x}\zeta^{(1,0)}(-1,1+x) + \frac{1}{x}\zeta^{(1,1)}(-2,1+x) - 2\zeta^{(1,1)}(-1,1+x), \tag{4.13a}$$

$$s^{\rm TE}(x) = -\frac{3}{4} - \frac{1}{3x} + \frac{2x}{3} + \frac{1}{2}\ln\frac{x}{2\pi} - 2\ln\Gamma(x) - \frac{6}{x^2}\psi^{(-3)}(x) + \frac{6}{x}\psi^{(-2)}(x), \tag{4.13b}$$

where $\psi^{(n)}$ are polygamma functions. It gives the correct limits for large x (strong coupling, low temperature)

$$x \gg 1: \quad s^{\rm TE}(x) \sim -\frac{3\zeta(3)}{4\pi^2x^2} + \frac{1}{45x^3} - \frac{1}{315x^5} + \frac{1}{525x^7} - \cdots, \tag{4.14a}$$

and for small x (weak coupling, high temperature)

$$x \ll 1: \quad s^{\rm TE}(x) \sim -\frac{1}{3x} + \frac{3}{4} - \frac{1}{2}\ln 2\pi x + \frac{2x}{3} - \frac{\pi^2}{24}x^2 + \ldots. \tag{4.14b}$$

The limit in (4.14a) corresponds to the strong-coupling result (3.6), while the limit in (4.14b) corresponds to the entropy derived from Eqs. (4.6) and (4.7). Figure 2 shows how the asymptotic limits are approached by the exact entropy. Note that the Nernst heat theorem is satisfied, in that the entropy vanishes at zero temperature, but this scalar entropy is always negative.

B. Finite coupling–TM mode

In the TM case, instead of a weak-coupling expansion, we are naturally led to a strong-coupling one, again in the

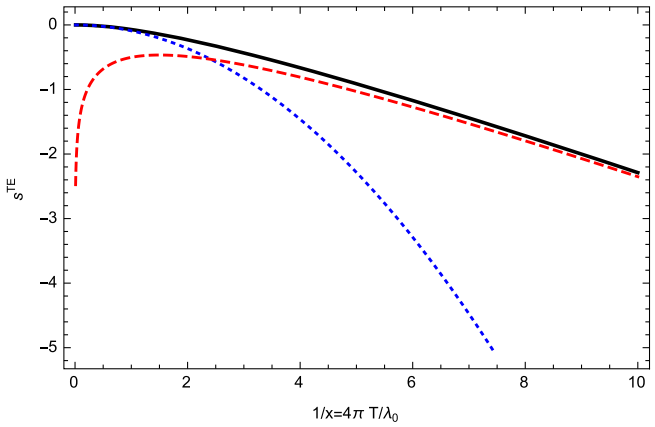

FIG. 2. The dimensionless scalar entropy for a single δ-function plate, which is the same as the TE electromagnetic entropy in the plasma model, shown as a solid black line, as a function of the temperature divided by the coupling strength. The dotted blue line shows the strong-coupling, low-temperature limit, while the dashed red line depicts the behavior at high temperature or weak coupling. The entropy satisfies the third law of thermodynamics, in that the entropy vanishes as the temperature goes to zero, but it is, surprisingly, always negative.

plasma model. It is convenient to subtract off the leading logarithm term from the first term in Eq. (2.7), i.e. $F^{\mathrm{TM}} = F_1 + F_2$, where, using Eq. (3.1),

$$F_1 = \frac{T}{2\pi}\sum_{m=0}^{\infty}{}' \cos(\zeta_m \tau)\int_0^\infty dk\, kJ_0(k\delta)\ln\left(1+\frac{2\zeta_m^2}{\lambda_0\kappa_m}\right), \tag{4.15a}$$

$$F_2 = \frac{T}{2\pi}\sum_{m=0}^{\infty}{}' \cos(\zeta_m \tau)\int_0^\infty dk\, kJ_0(k\delta)\ln\kappa_m. \tag{4.15b}$$

For simplicity we set $\tau = 0$ again. The integration in F_2 is evaluated using Eq. (3.2). In fact, this term is the negative of the strong-coupling limit for the TE mode, Eq. (3.6), so we write down without more ado

$$F_2 = -\frac{1}{8\pi\delta^3} - \frac{\zeta(3)}{4\pi}T^3. \tag{4.16}$$

F_1 is the same as the TE free energy (4.1) but with the substitution $\lambda_0/2 \to 2\zeta_m^2/\lambda_0$. Thus, here we naturally have a strong-coupling expansion. The first-order term in $1/\lambda_0$ is obtained, using Eq. (4.5), to be

$$F_1^{(1)} = \frac{1}{\pi^2\lambda_0\delta^4} - \frac{\pi^2}{15}\frac{T^4}{\lambda_0}. \tag{4.17a}$$

The second-order term is slightly more complicated, requiring use of the Euler-Maclaurin formula (3.4) and Borel summation; the result is

$$F_1^{(2)} = -\frac{9}{4\pi\lambda_0^2\delta^5} - \frac{12\zeta(5)}{\pi\lambda_0^2}T^5. \tag{4.17b}$$

The third-order term can again be done exactly, since it has only exponentials,

$$F_1^{(3)} = \frac{80}{\pi^2\lambda_0^3\delta^6} - \frac{t^6}{378\pi^2\lambda_0^3}, \tag{4.17c}$$

where we have now adopted a convenient abbreviation $t = 2\pi T$.

In general, we expand F_1 in powers of $1/\lambda_0$ as

$$F_1 = \frac{T}{2\pi}\sum_{m=1}^{\infty}\sum_{n=1}^{\infty}\frac{(-1)^{n+1}}{n}\left(\frac{2\zeta_m^2}{\lambda_0}\right)^n\int_0^\infty dk\, k\frac{J_0(k\delta)}{\kappa_m^n}, \tag{4.18}$$

where the integral is evaluated according to

$$\int_0^\infty \frac{dk\, kJ_0(k\delta)}{(k^2+\zeta_m^2)^{n/2}} = \delta^{n-2}\frac{n(|\zeta_m|\delta)^{1-n/2}K_{n/2-1}(|\zeta_m|\delta)}{2^{n/2}\Gamma(1+n/2)}, \quad n > \frac{1}{2}. \tag{4.19}$$

For a given n, we evaluate the m sum using the Euler-Maclaurin sum formula. In doing so, we encounter the finite sum

$$-\frac{1}{n+3}+\frac{1}{2}+\sum_{k=1}^{\infty}\frac{B_{2k}}{(2k)!}\frac{(-n-4+2k)!}{(-n-3)!} = \zeta(-n-2), \qquad \zeta(1-2k) = -\frac{B_{2k}}{2k}. \tag{4.20}$$

Thus, the nth term in the expansion of the free energy has the form

$$F_1^{(n)} = \frac{(-1)^{n-1}}{4\pi^2\delta^3}\left(\frac{4}{\lambda_0\delta}\right)^n\frac{\Gamma(n+\frac{1}{2})\Gamma(\frac{n+3}{2})}{\Gamma(\frac{n}{2}+1)} - \frac{t^3}{8\pi^2}y^n\frac{B_{n+3}}{n+3}\left(\frac{1}{n-2}-\frac{1}{n}\right), \qquad n > 2, \tag{4.21}$$

where $y = 1/x = 2t/\lambda_0$. Note that the divergent part is independent of temperature, and hence does not contribute to the entropy. [This expression agrees with the previous results (4.17) even for $n = 2$, where an appropriate limit must be understood.] We calculate the asymptotic sum appearing for the finite part using Borel summation, namely,

$$\sum_{n=3}^{\infty}F_{1f}^{(n)} = -\frac{t^3}{8\pi^2}\int_0^y\frac{du}{u^4}w(u)\left(\frac{y^2}{u^2}-1\right), \tag{4.22}$$

where

$$w(u)=\int_0^\infty \frac{dz}{z}e^{-z}\left[\frac{uz}{e^{uz}-1}-B_0-B_1uz-\frac{B_2}{2}(uz)^2-\frac{B_4}{4!}(uz)^4\right]$$
$$=\frac{u}{120}(-60-10u+u^3)-\ln u-\psi(1/u). \tag{4.23}$$

Here we have regarded the integrand as the analytic continuation of the Bernoulli series $\sum_{n=0}^{\infty}[B_{n+6}/(n+6)!](uz)^n$. The u integral in Eq. (4.22) can be carried out, with the explicit result, including the F_2 and the $n=1$ and $n=2$ terms, for the finite part of the TM free energy in terms of polygamma functions,

$$F_f^{\rm TM}=-\frac{t^3}{8\pi^2}\left[\frac{3}{2\pi^4x^2}\zeta(5)+\frac{1}{2\pi^2}\zeta(3)-\frac{x}{18}-\frac{x^2}{8}-\frac{16x^3}{225}\right.$$
$$+\frac{2x^3}{15}\ln x+\frac{24}{x^2}\psi^{(-5)}(x)-\frac{24}{x}\psi^{(-4)}(x)$$
$$\left.+10\psi^{(-3)}(x)-2x\psi^{(-2)}(x)\right]. \tag{4.24}$$

The divergent part of the free energy does not depend on T, so it does not contribute to the entropy. The latter can be written as

$$S^{\rm TM}(x)=-\frac{\partial F^{\rm TM}}{\partial T}=\frac{\lambda_0^2}{16\pi}s^{\rm TM}, \tag{4.25a}$$

where the dimensionless entropy is

$$s^{\rm TM}(x)=\frac{15\zeta(5)}{2\pi^4x^4}+\frac{3\zeta(3)}{2\pi^2x^2}-\frac{1}{9x}-\frac{1}{8}$$
$$-\frac{2}{15}x+2\ln\Gamma(x)+\frac{120}{x^4}\psi^{(-5)}(x)-\frac{120}{x^3}\psi^{(-4)}(x)$$
$$+\frac{54}{x^2}\psi^{(-3)}(x)-\frac{14}{x}\psi^{(-2)}(x). \tag{4.25b}$$

The behavior of this function for small x (small coupling, high temperature) is

$$s^{\rm TM}(x)\sim\frac{15\zeta(5)}{2\pi^4}\frac{1}{x^4}+\frac{3\zeta(3)}{2\pi^2}\frac{1}{x^2}-\frac{1}{9}\frac{1}{x}+\frac{1}{8}-\frac{2}{15}x+O(x^2),$$
$$x\ll 1, \tag{4.26a}$$

while the large x (large coupling, low temperature) expansion is

$$s^{\rm TM}(x)\sim\frac{3\zeta(3)}{4\pi^2}\frac{1}{x^2}+\frac{1}{15}\frac{1}{x^3}+\frac{15\zeta(5)}{4\pi^4}\frac{1}{x^4}+\frac{1}{63}\frac{1}{x^5}+O(x^{-6}),$$
$$x\gg 1. \tag{4.26b}$$

The similar appearance of the zeta functions in these two limits is remarkable. The entropy is plotted in Fig. 3. The comparison between the total self-entropy, $s=s^{\rm TE}+s^{\rm TM}$, and its TE and TM components is given in Fig. 4. It is clear that the latter dominates and results in an everywhere positive entropy. The negative TE entropy contributes equally to the TM entropy only for large x, where the entropy is very small. Therefore, the plasma model gives a physically satisfactory result: an everywhere positive self-entropy, which tends to zero at zero temperature.

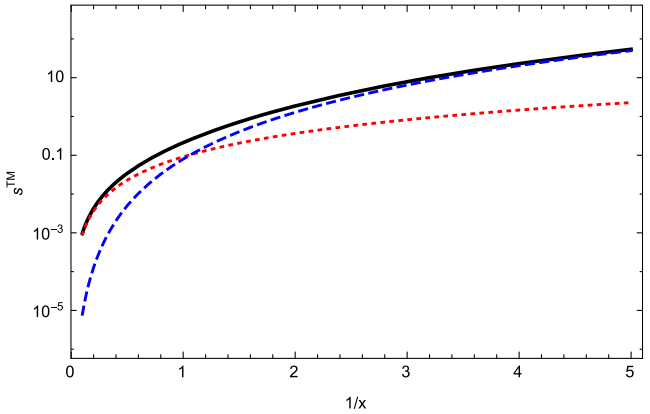

FIG. 3. Semilog plot of the transverse magnetic entropy $s^{\rm TM}$ as a function of $y=1/x=4\pi T/\lambda_0$ for the plasma model. It is compared with the leading asymptotic expansions for large and small x given in Eqs. (4.26), in the dotted and dashed lines, respectively. The TM entropy is always positive, and overwhelms the negative TE entropy seen in Fig. 2 except for large x.

C. Drude model

The above discussion, consistent with the approach in Ref. [13], uses a plasma-model type description of dispersion in the plate. However, were we to use the Drude model (which for metals is much more realistic) with the small damping factor ν and $\lambda=\lambda_0/(\zeta_m^2+\nu\zeta_m)$, the situation is more subtle. The affect on above calculations is only substantial for the $m=0$ contributions. For the TE mode

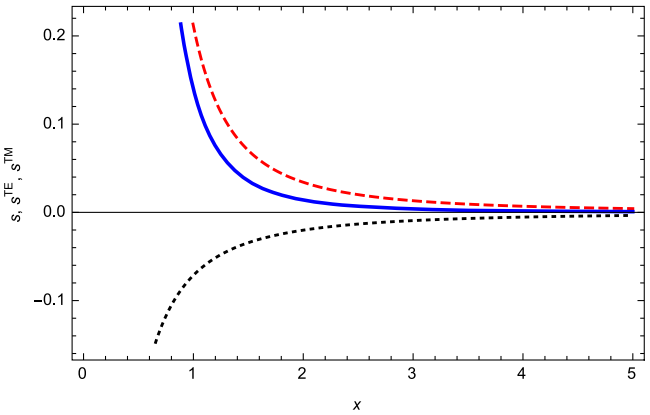

FIG. 4. The total self-entropy $s=s^{\rm TE}+s^{\rm TM}$ of a electromagnetic δ-function plate in the plasma model, plotted as a function of $x=\lambda_0/(4\pi T)$. Shown for comparison is the TM contribution (red, dashed line) and the TE contribution (black, dotted line).

part, it means that the term (4.3) would not be present, which leads, even in order λ_0, to a divergent $(1/\delta)$ contribution to the entropy. The TM $m=0$ mode is still vanishing. The resulting divergent contribution to the entropy appearing in the Drude model would be

$$S^D_{\rm div} = \frac{\lambda_0}{8\pi\delta} + \frac{\lambda_0^2}{32\pi}\ln\delta, \qquad T \gg \nu. \tag{4.27}$$

The Nernst theorem, that the entropy vanishes as $T \to 0$, is still satisfied, but there seems to be a problem for finite temperature, in that the entropy is no longer finite. As in the situation with realistic metals, the Drude model, while undoubtedly more physical, leads to some complications [21–23]. Investigations along these lines are continuing.

V. DISCUSSION

As expected, the electromagnetic self-entropy of a thin (δ-function) plate is positive, although the scalar or TE contribution is negative. But the total self-entropy of a perfectly conducting plate vanishes, so this by itself cannot resolve the negative interaction entropy encountered between a perfectly conducting plate and a perfectly conducting sphere, discussed in the Introduction and displayed in Fig. 1. However, we also must consider the self-entropy of the nanosphere. If we consistently regard the electric and magnetic polarizabilities, α and β, respectively, of the sphere as weak, Eq. (2.3) reduces, in the single-scattering approximation, to

$$F_b = -\frac{T}{2}\sum_{m=-\infty}^{\infty} {\rm Tr} V_b \mathbf{\Gamma}_0, \quad V_b = 4\pi b\delta(\mathbf{r}), \quad b=\alpha,\beta, \tag{5.1}$$

for an isotropic nanosphere at the origin. We can write the free (vacuum) Green's dyadic as in Eq. (A13), which leads immediately to the electric free energy

$$F_\alpha = \frac{T\alpha}{R}\sum_{m=-\infty}^{\infty} \zeta_m^2 e^{-|\zeta_m|R}\Big|_{R\to 0}. \tag{5.2}$$

Here R is the spatial point-splitting quantity. The sum is written in terms of a hyperbolic cotangent, which is then expanded for small R,

$$F_\alpha = \frac{2\alpha}{\pi R^4} - \frac{2\alpha}{15}\pi^3 T^4, \tag{5.3}$$

and the magnetic free energy has the same expression with $\alpha \to \beta$. Adding the electric and magnetic free energies for a perfectly conducting sphere of radius a, where $\alpha = -2\beta = a^3$, we obtain for the entropy of such an object

$$S_{\rm pcs} = \frac{4}{15}(\pi a T)^3. \tag{5.4}$$

The result (5.4) was first derived by Balian and Duplantier [24]. The self-entropy of a conducting sphere is positive, and precisely cancels the most negative value of the interaction entropy (1.1). So the entropy of the nanosphere-plate system is always positive, being zero at zero separation.

More generally, if $\alpha \neq \beta$, the sum of the self-entropy of the sphere and the interaction entropy of the sphere with the plate is

$$S \geq \frac{16\pi^3}{45} T^3(\alpha + 2\beta). \tag{5.5}$$

This will be positive if $\alpha + 2\beta > 0$, so the perfectly conducting case is the limiting value to avoid negative entropy. The Drude model, where $\beta = 0$, would be strictly positive.

For the case of the interaction between two atoms, the situation seems even more clear-cut. In that case, for two isotropic atoms separated by a short distance Z the interaction entropy is given by Ref. [9],

$$S = \frac{(4\pi T)^5}{5040 Z}[11(\alpha_1\alpha_2 + \beta_1\beta_2) + 5(\alpha_1\beta_2 + \alpha_2\beta_1)]. \tag{5.6}$$

Isotropy has resulted in cancellation of the leading term in $(4\pi ZT)$. Whatever the sign of this term, it always seems much smaller in magnitude than the sum of the self-entropies of the nanoparticles. The size of the interaction entropy relative to the self-entropy is

$$\frac{T^2}{Z}\alpha \sim (Ta)^2\frac{a}{Z}. \tag{5.7}$$

Ta is typically a very small number: for $a = 10^{-8}$ cm, at room temperature $Ta \sim 10^{-5}$. And a/Z is necessarily a small number in order that the dipole approximation be valid.

VI. CONCLUSIONS

In this paper, we have calculated the self-entropy of a thin (δ-function) electromagnetic plate, with a general dispersive coupling λ. We assume a plasmalike dispersion relation and examine the TE and TM mode in detail, computing the free energy from a weak-coupling expansion in the first instance and a strong-coupling expansion in the second. In each case we get a closed form result for the entropy. The TE contribution to the entropy of the plate is always negative while the TM is positive, and yields a positive total self-entropy. In strong coupling, the entropy vanishes.

In order to understand how the entropy of the system composed on a polarizable nanoparticle interacting via quantum fluctuations with a conducting plate, we must therefore consider the self-entropy of the nanoparticle

itself. At least for the case of a conducting sphere, the later is just sufficient to render the total entropy positive for all separation distances.

One might have thought that this question is moot, because the entropy of empty space, discussed in the Appendix, of course overwhelms any small negative entropy between atoms or between atoms and surfaces. However, the latter entropy is quite distinct from the system being studied, so it is gratifying that positive entropy emerges when the system by itself is considered.

The observability of negative entropy might also be questioned: It is not easy to devise experimental signatures of entropy, which, although physical, is primarily a theoretical construct. Perhaps what is more relevant is the slope of the entropy, or the specific heat,

$$C_v = T\frac{\partial S}{\partial T}. \tag{6.1}$$

So the signature of something unusual is nonmonotonicity of the entropy, which, of course, is exhibited in the interaction between a nanosphere and a conducting plate. For further discussion of negative specific heats in this and related contexts, see Refs. [25,26].

Elsewhere we will investigate the self-entropy of a δ-function sphere to complete this self-entropy project. We expect congruence with the results found here in the strong-coupling (perfectly conducting) limit. We also would like to explore further the connection between negative entropy and Casimir repulsion [27], both of which involve nonmonotonicity of the free energy. We hope experimental evidence for both of these phenomena may soon be forthcoming.

ACKNOWLEDGMENTS

We thank the Julian Schwinger Foundation for partial support of this research. The beginnings of this research were carried out while K. A. M. was on sabbatical at Laboratoire Kastler Brossel. He thanks CNRS and the Simons Foundation for support. He also thanks the OU College of Arts and Sciences for travel support. P. P. acknowledges support from the Norwegian Research Council, Project No. 250346. We thank Gert-Ludwig Ingold, Taylor Murphy, Jacob Tice, and Stephen Fulling for helpful discussions.

APPENDIX: VACUUM STRESS TENSOR

1. Lorentz invariant regularization

The scalar vacuum Green's function, for Euclidean time, is

$$G_0(R, t_E - t'_E) = \int_{-\infty}^{\infty}\frac{d\zeta}{2\pi}\frac{e^{i\zeta(t-t')_E - |\zeta|R}}{4\pi R} = \frac{1}{4\pi^2}\frac{1}{R^2 + (t-t')_E^2}, \tag{A1}$$

where $R^2 = (r-r')^2$, $t_E - t'_E = -i(t-t')$, and ζ is the imaginary frequency, $\omega = i\zeta$. G_0 is just the Euclidean four-dimensional (4D) Coulomb propagator,

$$G_0(\mathcal{R}) = \frac{1}{4\pi^2\mathcal{R}^2}, \qquad \mathcal{R}^2 = R^2 + (t-t')_E^2 = R^2 - (t-t')^2. \tag{A2}$$

The stress tensor may be taken to be the canonical one, since the conformal term will not contribute,[2]

$$\langle T^{\mu\nu}\rangle = \left[\partial^\mu\partial'^\nu - \frac{1}{2}g^{\mu\nu}\partial_\lambda\partial'^\lambda\right]\frac{1}{4\pi^2\mathcal{R}^2}. \tag{A3}$$

After differentiation, we get a traceless result coinciding with that of Christensen's [14]

$$\langle T^{\mu\nu}\rangle = \frac{1}{2\pi^2\delta^4}\left[g^{\mu\nu} - 4\frac{\delta^\mu\delta^\nu}{\delta^2}\right], \qquad \delta^\mu = (i\tau, \boldsymbol{\rho}),$$
$$\delta^2 = \delta^\mu\delta_\mu = \rho^2 + \tau^2, \tag{A4}$$

by taking the coincidence limit $r' \to \mathbf{r} + \boldsymbol{\rho}$, $t' \to t + i\tau$ with splittings in time and space $\boldsymbol{\rho}, \tau \to 0$. Note that the energy density possesses the familiar time-splitting and space-splitting Weyl divergent form

$$\langle T^{00}\rangle = -\frac{1}{2\pi^2}\frac{\rho^2 - 3\tau^2}{(\rho^2+\tau^2)^3}. \tag{A5}$$

In general, the stress tensor (A4) is neither diagonal nor rotationally invariant, which seems unacceptable. Schwinger [28] would have argued that in point splitting, you should average over all directions, so that

$$\langle\tau\rho_x\rangle = \langle\rho_x\rho_y\rangle = 0, \text{etc.}, \quad \text{and} \quad \langle\rho_x^2\rangle = \langle\rho_y^2\rangle = \langle\rho_z^2\rangle = \frac{1}{3}\rho^2, \tag{A6}$$

and then the stress tensor becomes diagonal and has the form characteristic of radiation,

$$\langle T^{\mu\nu}\rangle = \frac{1}{2\pi^2}\frac{\tau^2 - \rho^2/3}{(\tau^2+\rho^2)^3}(g^{\mu\nu} + 4\eta^\mu\eta^\nu), \qquad \eta^\mu = (1,0,0,0). \tag{A7}$$

This form, for τ splitting, is also given in Christensen [14]. This is still not Lorentz invariant, but it would be if the cutoff is made 4D rotationally invariant, $\tau^2 = \rho^2/3$, just like the spatial point splittings (A6). It is in this sense that the regulated (consistent with required Lorentz symmetry) vacuum expectation value of the stress tensor is zero, $\langle T^{\mu\nu}\rangle = 0$. We can turn this argument around and

[2]Note we are working in Minkowski space; the time regulator is taken to be Euclidean, however.

"understand" why there is the factor of −3 between the time-splitting and space-splitting results for the Weyl divergent volume term (A5).

2. Finite temperature

For $T > 0$ Green's function is expressed as a sum over Matsubara frequencies $\zeta_m = 2\pi m T$,

$$G_T(R, t-t') = T\sum_{m=-\infty}^{\infty} \frac{e^{i\zeta_m (t-t')_E - |\zeta_m| R}}{4\pi R} = \frac{T}{8\pi R}\{\coth \pi T[R - i(t-t')_E] + \coth \pi T[R + i(t-t')_E]\}, \tag{A8}$$

which reduces to the zero-temperature Green's function G_0 as $T \to 0$. We compute the energy density using Eq. (A3),

$$\langle T^{00}\rangle_T = -\frac{\pi T^3}{4R}\frac{\cosh \pi T(\rho + i\tau)}{\sinh^3 \pi T(\rho + i\tau)} + (\tau \to -\tau) \to -\frac{1}{2\pi^2}\frac{\rho^2 - 3\tau^2}{(\rho^2+\tau^2)^3} + \frac{\pi^2 T^4}{30}, \tag{A9}$$

where we have now taken the coincidence limit $R \to \rho$, $t - t' \to i\tau$ with $\rho, \tau \to 0$. The correction to the zero-temperature divergent term is one-half the usual Planck black-body radiation density.

From the thermodynamic relation $\frac{\partial u}{\partial T} = T\frac{\partial s}{\partial T}$, we deduce the entropy density s and the free energy density f,

$$s = -\frac{\partial f}{\partial T} = \frac{4\pi^2 T^3}{90}, \qquad f = \frac{1}{2\pi^2}\frac{3\tau^2 - \rho^2}{(\rho^2+\tau^2)^3} - \frac{\pi^2 T^4}{90}. \tag{A10}$$

Other components of the vacuum expectation value of the stress tensor are easily deduced from the energy density provided we again use the three-dimensional averaging procedure. For example,

$$\langle T_{11}\rangle_T = \frac{1}{2}(\partial^0\partial'^0 + \partial_1\partial'_1 - \boldsymbol{\nabla}_\perp\cdot\boldsymbol{\nabla}'_\perp)G_T = \frac{1}{3}\langle T^{00}\rangle_T, \tag{A11}$$

because the spatial derivatives average to $-\frac{1}{3}\boldsymbol{\nabla}\cdot\boldsymbol{\nabla}'$. Then we deduce

$$\langle T^{\mu\nu}\rangle_T = \left[\frac{1}{2\pi^2}\frac{\tau^2 - \rho^2/3}{(\rho^2+\tau^2)^3} + \frac{\pi^2 T^4}{90}\right](g^{\mu\nu} + 4\eta^\mu\eta^\nu). \tag{A12}$$

3. Electromagnetic vacuum stress tensor

The corresponding construction for the electromagnetic field proceeds in a very similar manner. In that case, the free Green's dyadic is

$$\boldsymbol{\Gamma}_0(\mathbf{r}, \mathbf{r}') = (\boldsymbol{\nabla}\boldsymbol{\nabla} - \mathbf{1}\nabla^2)\frac{e^{-|\zeta|R}}{4\pi R}, \qquad \mathbf{R} = \mathbf{r} - \mathbf{r}', \tag{A13}$$

so when the identification $i\langle \mathbf{E}(\mathbf{r})\mathbf{E}(\mathbf{r}')\rangle = \boldsymbol{\Gamma}_0(\mathbf{r}, \mathbf{r}')$ is made, the point-split regulated energy density, for example, is

$$u = \int \frac{d\zeta}{2\pi} e^{i\zeta\tau}\frac{1}{2}\mathrm{Tr}\left(\boldsymbol{\Gamma}_0 - \frac{1}{\zeta^2}\boldsymbol{\nabla}\times\boldsymbol{\Gamma}_0\times\overleftarrow{\boldsymbol{\nabla}}'\right). \tag{A14}$$

The electric and magnetic contributions are equal because

$$\mathrm{Tr}\boldsymbol{\Gamma}_0 = -\mathrm{Tr}\frac{1}{\zeta^2}\boldsymbol{\nabla}\times\boldsymbol{\Gamma}_0\times\overleftarrow{\boldsymbol{\nabla}}' = -\frac{\zeta^2}{2\pi R}e^{-|\zeta|R}. \tag{A15}$$

The integral over ζ is easily worked out, with the result that

$$u = -\frac{1}{\pi^2}\frac{\rho^2 - 3\tau^2}{(\rho^2+\tau^2)^3}, \tag{A16}$$

which is twice the scalar result (A5). Since the stress tensor is traceless, the other components of the vacuum expectation value of the stress tensor must be twice the scalar result (A4) as well. The finite temperature form must also be twice that given in Eq. (A12) because the differential operator appearing in the scalar energy density construction is

$$\partial^0\partial^{0\prime} - \frac{1}{2}\partial_\lambda\partial^{\lambda\prime} = \frac{1}{2}\partial^0\partial^{0\prime} + \frac{1}{2}\boldsymbol{\nabla}\cdot\boldsymbol{\nabla}' \to -\zeta^2, \tag{A17}$$

just the multiplier we see in the electromagnetic case. Indeed, this is borne out by explicit calculation.

[1] V. B. Bezerra, G. L. Klimchitskaya, V. M. Mostepanenko, and C. Romero, Violation of the Nernst heat theorem in the theory of thermal Casimir force between Drude metals, Phys. Rev. A **69**, 022119 (2004).

[2] I. Brevik, J. B. Aarseth, J. S. Høye, and K. A. Miton, On the temperature dependence of the Casimir effect, Phys. Rev. E **71**, 056101 (2005).

[3] I. Brevik, S. A. Ellingsen, and K. A. Milton, Thermal corrections to the Casimir effect, New J. Phys. **8**, 236 (2006).

[4] V. B. Bezerra, G. L. Klimchitskaya, V. M. Mostepanenko, and C. Romero, Lifshitz theory of atom-wall interaction with applications to quantum reflection, Phys. Rev. A **78**, 042901 (2008).

[5] A. Canaguier-Durand, P. A. Maia Neto, A. Lambrecht, and S. Reynaud, Thermal Casimir Effect in the Plane-Sphere Geometry, Phys. Rev. Lett. **104**, 040403 (2010).
[6] A. Canaguier-Durand, P. A. Maia Neto, A. Lambrecht, and S. Reynaud, Thermal Casimir effect for Drude metals in the plane-sphere geometry, Phys. Rev. A **82**, 012511 (2010).
[7] P. Rodriguez-Lopez, Casimir energy and entropy in the sphere-sphere geometry, Phys. Rev. B **84**, 075431 (2011).
[8] P. Rodriguez-Lopez, Casimir energy and entropy between perfect metal sphere, Quantum field theory under the influence of external conditions (QFEXT11), Int. J. Mod. Phys. Conf. Ser. **14**, 475 (2012).
[9] K. A. Milton, R. Guérout, G.-L. Ingold, A. Lambrecht, and S. Reynaud, Negative Casimir entropies in nanoparticle interactions, J. Phys. Condens. Matter **27**, 214003 (2015).
[10] G.-L. Ingold, S. Umrath, M. Hartmann, R. Guérout, A. Lambrecht, S. Reynaud, and K. A. Milton, Geometric origin of negative Casimir entropies: A scattering-channel analysis, Phys. Rev. E **91**, 033203 (2015).
[11] S. Umrath, M. Hartmann, G.-L. Ingold, and P. A. Maia Neto, Disentangling geometric and dissipative origins of negative Casimir entropies, Phys. Rev. E **92**, 042125 (2015).
[12] K. A. Milton, Y. Li, P. Kalauni, P. Parashar, R. Guérout, G.-L. Ingold, A. Lambrecht, and S. Reynaud, Negative entropies in Casimir and Casimir-Polder interactions, arXiv:1605.01073 [Fortschr. Phys. (to be published)].
[13] P. Parashar, K. A. Milton, K. V. Shajesh, and M. Schaden, Electromagnetic semitransparent δ-function plate: Casimir interaction energy between parallel infinitesimally thin plates, Phys. Rev. D **86**, 085021 (2012).
[14] S. M. Christensen, Vacuum expectation value of the stress tensor in an arbitrary curved background: The covariant point separation method, Phys. Rev. D **14**, 2490 (1976).
[15] G. Barton, Casimir effects in monatomically thin insulators polarizable perpendicularly: Nonretarded approximation, New J. Phys. **15**, 063028 (2013).
[16] M. Bordag, Monoatomically thin polarizable sheets, Phys. Rev. D **89**, 125015 (2014).
[17] K. A. Milton, P. Parashar, E. K. Abalo, F. Kheirandish, and K. Kirsten, Investigations of the torque anomaly in an annular sector. II. Global calculations, electromagnetic case, Phys. Rev. D **88**, 045030 (2013).
[18] K. A. Milton, K. V. Shajesh, S. A. Fulling, and P. Parashar, How does Casimir energy fall? IV. Gravitational interaction of regularized quantum vacuum energy, Phys. Rev. D **89**, 064027 (2014).
[19] K. A. Milton, S. A. Fulling, P. Parashar, P. Kalauni, and T. Murphy, Stress tensor for a scalar field in a spatially varying background potential: Divergences, renormalization, anomalies, and Casimir forces, Phys. Rev. D **93**, 085017 (2016).
[20] S. A. Ellingsen, I. Brevik, J. S. Høye, and K. A. Milton, Temperature correction to Casimir-Lifshitz free energy at low temperatures: Semiconductors, Phys. Rev. E **78**, 021117 (2008).
[21] K. A. Milton, I. Brevik, and S. Å. Ellingsen, Thermal issues in Casimir forces between conductors and semiconductors, Phys. Scr. **T151**, 014070 (2012).
[22] J. S. Høye, I. Brevik, J. B. Aarseth, and K. A. Milton, Does the transverse electric zero mode contribute to the Casimir effect for a metal?, Phys. Rev. E **67**, 056116 (2003).
[23] M. Boström and B. E. Sernelius, Thermal Effects on the Casimir Force in the 0.1–5 μm Range, Phys. Rev. Lett. **84**, 4757 (2000).
[24] R. Balian and B. Duplantier, Electromagnetic waves near perfect conductors. 2. Casimir effect, Ann. Phys. (N.Y.) **112**, 165 (1978).
[25] B. Spreng, G.-L. Ingold, and U. Weiss, Anomalies in the specific heat of a free damped particle: The role of the cutoff in the spectral density of the coupling, Phys. Scr. **T165**, 014028 (2015).
[26] G.-L. Ingold, A. Lambrecht, and S. Reynaud, Quantum dissipative Brownian motion and the Casimir effect, Phys. Rev. E **80**, 041113 (2009).
[27] K. A. Milton, E. K. Abalo, P. Parashar, N. Pourtolami, I. Brevik, S. Å. Ellingsen, S. Y. Buhmann, and S. Scheel, Casimir-Polder repulsion: Three-body effects, Phys. Rev. A **91**, 042510 (2015).
[28] J. Schwinger, Field Theory Commutators, Phys. Rev. Lett. **3**, 296 (1959).